

Tension estimation method using natural frequencies for cable equipped with two dampers

Aiko Furukawa^{*1}, Kenki Goda¹ and Tomohiro Takeichi²

¹Department of Urban Management, Graduate School of Engineering, Kyoto University,
Kyotodaigaku-katsura, Nishikyo-ku, Kyoto-shi, Kyoto 615-8540, Japan

²Kobelco Wire Company, Ltd., 10-1, Nakahama-cho. Amagasaki-shi, Hyogo 660-0091, Japan

(Received November 17, 2023, Revised December 17, 2023, Accepted December 20, 2023)

Abstract. In cable structure maintenance, particularly for cable-stayed bridges, cable safety assessment relies on estimating cable tension. Conventionally, in Japan, cable tension is estimated from the natural frequencies of the cable using the higher-order vibration method. In recent years, dampers have been installed on cables to reduce cable vibrations. Because the higher-order vibration method is a method for damper-free cables, the damper must be removed to measure the natural frequencies of a cable without a damper. However, cables on some cable-stayed bridges have two dampers: one on the girder side and another on the tower side. Notably, removing and reinstalling the damper on the tower side are considerably more time- and labor-intensive. This paper introduces a tension estimation method for cables with two dampers, using natural frequencies. The proposed method was validated through numerical simulation and experiment. In the numerical tests, without measurement error in the natural frequencies, the maximum estimation error among 100 models was 3.3%. With measurement error of 2%, the average estimation error was within 5%, with a maximum error of 9%. The proposed method has high accuracy because the higher-order vibration method for a damper-free cable still has an estimation error of 5%. The experimental verification emphasizes the importance of accurate damper modeling, highlighting potential discrepancies between existing damper design formula and actual damper behavior. By revising the damper formula, the proposed method achieved accurate cable tension estimation, with a maximum estimation error of approximately 10%.

Keywords: cable tension estimation; damper modeling; natural frequencies; two dampers

1. Introduction

In cable structure maintenance in Japan, it is mandatory to evaluate the cable tension once every 5 years. The estimation of cable tension primarily relies on the natural frequencies of the cables, employing either the vibration method (Shinke *et al.* 1980, Zui *et al.* 1996) or higher-order vibration method (Yamagiwa *et al.* 2000).

The vibration method, which is rooted in string theory, faces the problem of the actual bridge cable not being a string and having bending stiffness. To account for this, a correlation factor is introduced, necessitating the prior determination of bending stiffness. However, the exact bending

*Corresponding author, Associate Professor, E-mail: furukawa.aiko.3w@kyoto-u.ac.jp

stiffness is difficult to determine because bridge cables are typically stranded wires, and a theoretical formula for calculating the bending stiffness of stranded wires does not exist.

Conversely, the higher-order vibration method is based on tensioned Euler–Bernoulli beam theory. The natural frequency of a cable is expressed as a function of tension and bending stiffness. Consequently, the higher-order vibration method allows for the simultaneous estimation of tension and bending stiffness from natural frequencies, eliminating the need of pre-evaluating the bending stiffness. Therefore, this method is commonly employed in current engineering practice.

Numerous studies have investigated methodologies for estimating cable tension, including approaches that address intricate boundary conditions (Chen *et al.* 2016, 2018, Yan *et al.* 2019), the handling of uncertain boundary conditions in short cables by introducing an additional mass block (Li *et al.* 2021), strategies addressing inclined cables (Ma 2017, Kim and Park 2007), a methodology addressing cables with flexible supports (Foti *et al.* 2020), an approach tackling environmental temperature variations (Ma *et al.* 2021), techniques for two cables connected by an intersection clamp (Furukawa *et al.* 2022c, f, g), a method incorporating power spectrum and cepstrum analysis (Feng *et al.* 2010), an approach using finite element analysis (Gan *et al.* 2019), a methodology employing a genetic algorithm and particle swarm optimization (ZarbaF *et al.* 2017), a technique leveraging neural networks (ZarbaF *et al.* 2018), a method employing deep learning (Jeong *et al.* 2020), and a noncontact vision-based approach (Liu *et al.* 2023).

In recent times, the aerodynamic vibration of cables has been increasingly attracting attention. To mitigate cable vibration, dampers are deployed on cables. The installation of dampers alters the cable's natural frequencies. Consequently, the damper must be temporarily removed to estimate the cable tension using vibration and higher-order vibration methods. After the cable vibration is measured without the damper, the damper is reinstalled. Owing to the time-consuming and labor-intensive nature of this process, there is demand for a tension estimation method that is applicable to cables equipped with dampers.

Previous studies on cables with dampers have predominantly focused on optimizing damper design to suppress cable vibration (Pacheco *et al.* 1993, Krenk 2020, Tabatabai and Mehrabi 2000, Lazar *et al.* 2016, Shi and Zhu 2018, Javanbakht *et al.* 2019, Izzi *et al.* 2016), whereas few studies have investigated tension estimation methods. To date, scant attention has been given to the development of tension estimation methods specifically tailored to cables with dampers.

Shan *et al.* (2019) proposed a tension estimation approach for a cable with an additional damper, assuming a viscous shear damper with a known spring constant and damping coefficient. However, obtaining accurate values for the damper's spring constant and damping coefficient in advance is not always feasible.

Using a different approach, Hou *et al.* (2020) introduced a cable tension estimation method employing the substructure isolation method. By employing virtual supports, this method isolates the cable section without a damper. However, the installation and removal of virtual supports are time-consuming and labor-intensive.

Tension estimation methods for cables with a single damper, specifically positioned on the girder side, have been developed. Using the tensioned Euler–Bernoulli beam theory, theoretical equations for cable tension estimation have been developed from natural frequencies (Furukawa *et al.* 2021a, 2022b, d), and from natural frequencies and mode shapes (Furukawa *et al.* 2022e). In these studies, the damper was represented by a complex spring, wherein the real part of the spring constant denoted the damper's stiffness, and the imaginary part represented the damping terms attenuating the vibration. Notably, the cable's bending stiffness and damper parameters did not require advance determination; instead, they could be simultaneously estimated with the cable tension.

Despite these results, certain cable-stayed bridge cables incorporate two dampers—one on the girder side and another one on the tower side—leading to more time- and labor-intensive damper removal and reinstallation. In this context, this paper introduces a tension estimation method for a cable with two dampers. In a previous study addressing tension estimation for cables with two dampers, Yan *et al.* (2020) proposed a method for cables with two intermediate supports (dampers), and modeled the damper as a spring. This approach assumes that the damper's spring constants are known a priori and ignores the damping terms attenuating vibration. However, obtaining the damper's spring constants in advance and ignoring the damping terms are impractical. This study employed the tensioned Euler–Bernoulli beam theory for cable modeling and complex springs for damper modeling. Theoretical equations for estimating the cable tension, cable bending stiffness, and dampers' complex spring constants from natural frequencies were derived, eliminating the need for the prior determination of the cable bending stiffness and dampers' complex spring constants. The proposed method was validated through numerical simulation and experiment.

This study used a high-damping rubber damper in the experiments, and the authors identified a problem related to damper modeling errors. As is widely recognized, dampers exhibit frequency dependence (Weber and Distl 2015). Nevertheless, the design formula for the high-damping rubber damper remains independent of the frequency. Because this study considered a cable with two dampers, the effect of damper modeling errors on the estimation accuracy is more pronounced compared with the case involving a single damper. To address this issue, this study refined the damper formula and elucidated the significance of accurate damper modeling by systematically comparing the estimation accuracy of different damper formulas.

The rest of this paper is structured as follows. Section 2 describes the tension estimation method for a cable with two dampers. In Section 3, the numerical verification of 100 numerical models is presented. The natural frequencies of a cable with two dampers were calculated for 100 models and input into the proposed method. The estimated results were compared to the assumed true values, and their accuracy and validity are discussed. Section 4 presents the experimental verification and discusses the accuracy of the proposed method and importance of accurate damper modeling.

2. Proposed method for estimating tension of cable with two dampers

2.1 Definition of coordinate axes and parameters

This paper proposes a method for estimating the tension of a cable with two dampers. Fig. 1 shows the analytical model. The two dampers divide the cable into three sections. Each section ($d = 1, 2, 3$) has a coordinate axis x_d , and the deflection at coordinate x_d at time t is defined as $y_d(x_d, t)$. The cable length is L , and the length of each section is l_d . The cable is modeled as a tensioned Euler–Bernoulli beam, and both ends are assumed to have fixed support. The tension T , bending stiffness EI , cross-sectional area A , and density ρ are assumed to be uniform throughout the cable. The dampers are modeled as complex springs, and their spring constants are k_1^* and k_2^* , respectively.

2.2 Derivation of constraint equation for tension estimation

The deflection of a cable for each section follows the vibration equation for a tensioned Euler–

Bernoulli beam

$$\rho A \frac{\partial^2 y_d(x_d, t)}{\partial t^2} - T \frac{\partial^2 y_d(x_d, t)}{\partial x_d^2} + EI \frac{\partial^4 y_d(x_d, t)}{\partial x_d^4} = 0 \quad (d = 1, 2, 3) \quad (1)$$

Eq. (1) can be solved using the variable separation method; $y_d(x_d, t)$ is expressed as follows

$$y_d(x_d, t) = Y_d(x_d) \exp(2\pi j f t) \quad (2)$$

where $Y_d(x_d)$ is the modal function, j is the imaginary unit, and f is the frequency. By substituting Eq. (2) into Eq. (1), a general solution for the modal function $Y_d(x_d)$ can be obtained as follows:

$$Y_d(x_d) = C_{d1} \cos \alpha x_d + C_{d2} \sin \alpha x_d + C_{d3} \exp(\beta x_d) + C_{d4} \exp(-\beta x_d) \quad (3)$$

where C_{d1} , C_{d2} , C_{d3} , and C_{d4} are integral constants; α and β are expressed by Eqs. (4) and (5), respectively.

$$\alpha = \sqrt{\sqrt{\left(\frac{T}{2EI}\right)^2 + \frac{\rho A (2\pi f)^2}{EI}} - \frac{T}{2EI}} \quad (4)$$

$$\beta = \sqrt{\sqrt{\left(\frac{T}{2EI}\right)^2 + \frac{\rho A (2\pi f)^2}{EI}} + \frac{T}{2EI}} \quad (5)$$

There are 12 integral constants (C_{d1} , C_{d2} , C_{d3} , and C_{d4} for $d = 1, 2, 3$), and thus 12 boundary conditions are required.

First, the following equations are obtained because both ends of the cable have fixed supports.

$$Y_1(0) = 0 \quad (6)$$

$$\frac{dY_1(0)}{dx_1} = 0 \quad (7)$$

$$Y_3(l_3) = 0 \quad (8)$$

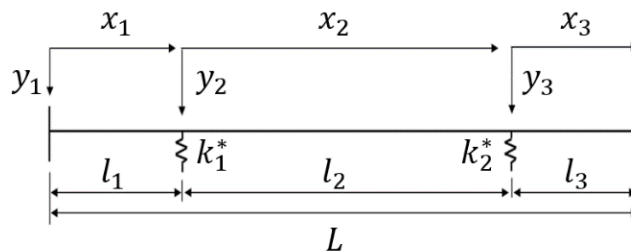


Fig. 1 Analytical model of a cable with two dampers

$$\frac{dY_3(l_3)}{dx_3} = 0 \tag{9}$$

Then, the following equations are obtained at the damper positions.

$$Y_1(l_1) = Y_2(0) \tag{10}$$

$$\frac{dY_1(l_1)}{dx_1} = \frac{dY_2(0)}{dx_2} \tag{11}$$

$$\frac{d^2Y_1(l_1)}{dx_1^2} = \frac{d^2Y_2(0)}{dx_2^2} \tag{12}$$

$$EI \frac{d^3Y_1(l_1)}{dx_1^3} - EI \frac{d^3Y_2(0)}{dx_2^3} = k_1^* Y_1(l_1) \tag{13}$$

$$Y_2(l_2) = Y_3(0) \tag{14}$$

$$\frac{dY_2(l_2)}{dx_2} = \frac{dY_3(0)}{dx_3} \tag{15}$$

$$\frac{d^2Y_2(l_2)}{dx_2^2} = \frac{d^2Y_3(0)}{dx_3^2} \tag{16}$$

$$EI \frac{d^3Y_2(l_2)}{dx_2^3} - EI \frac{d^3Y_3(0)}{dx_3^3} = k_2^* Y_2(l_2) \tag{17}$$

Eqs. (10)-(12) and (14)-(16) are continuity conditions, and Eqs. (13) and (17) are the equations of the equilibrium of forces, where k_1^* and k_2^* are the complex spring constants of the two dampers. Thus, 12 equations were developed for 12 integral constants. By substituting Eq. (3) into Eqs. (6)-(17) and rearranging, a simultaneous linear equation for 12 integral constants is obtained.

$$[\mathbf{D}]\{\mathbf{C}\} = \{\mathbf{0}\} \tag{18}$$

where $\{\mathbf{C}\} = \{C_{11} \cdots C_{14} \ C_{21} \cdots C_{24} \ C_{31} \cdots C_{34}\}^T$, and $[\mathbf{D}]$ is a coefficient matrix. For Eq. (18) to have a non-zero vector solution, the determinant of the coefficient matrix $[\mathbf{D}]$ must be zero.

$$\det[\mathbf{D}] = 0 \tag{19}$$

Eq. (19) can be rewritten as follows

$$G_1 \sin \alpha L + G_2 \cos \alpha L + G_3 = 0 \tag{20}$$

where G_1 , G_2 , and G_3 are the functions, including $\cos \alpha l_d$, $\sin \alpha l_d$, $\exp(\beta l_d)$, and $\exp(-\beta l_d)$ ($d = 1, 2, 3$). As expressed by Eqs. (4) and (5), α and β depend on the frequency f . The frequency f at which Eq. (20) holds is the natural frequency, and there exists an infinite number of natural frequencies satisfying Eq. (20). By arranging the natural frequencies in ascending order, the i^{th} natural frequency is defined as f_i . In the following text, the variables corresponding to the i^{th} natural frequency f_i are denoted by subscript i .

The magnitudes of G_{i1} and G_{i2} in Eq. (20) are different depending on the mode, and thus normalization is carried out as follows

$$\frac{G_{1i}}{\sqrt{G_{1i}^2 + G_{2i}^2}} \sin \alpha_i L + \frac{G_{2i}}{\sqrt{G_{1i}^2 + G_{2i}^2}} \cos \alpha_i L + \frac{G_{3i}}{\sqrt{G_{1i}^2 + G_{2i}^2}} = 0 \quad (21)$$

Notably, the natural frequency f_i satisfying Eq. (20) is a complex value because Eqs. (13) and (17) include complex spring constants, namely, k_1^* and k_2^* . Therefore, variable α_i becomes a complex value. Here, the authors divide the variable α_i into real and imaginary parts. Then, $\sin \alpha_i L$ and $\cos \alpha_i L$ in Eq. (21) are divided into real and imaginary parts, as follows

$$\begin{aligned} \sin \alpha_i L &= \sin(\operatorname{Re}(\alpha_i) + j\operatorname{Im}(\alpha_i))L \\ &= \sin(\operatorname{Re}(\alpha_i)L) (e^{\operatorname{Im}(\alpha_i)L} + e^{-\operatorname{Im}(\alpha_i)L})/2 + j \cos(\operatorname{Re}(\alpha_i)L) (e^{\operatorname{Im}(\alpha_i)L} - e^{-\operatorname{Im}(\alpha_i)L})/2 \end{aligned} \quad (22)$$

$$\begin{aligned} \cos \alpha_i L &= \cos(\operatorname{Re}(\alpha_i) + j\operatorname{Im}(\alpha_i))L \\ &= \cos(\operatorname{Re}(\alpha_i)L) (e^{\operatorname{Im}(\alpha_i)L} + e^{-\operatorname{Im}(\alpha_i)L})/2 - j \sin(\operatorname{Re}(\alpha_i)L) (e^{\operatorname{Im}(\alpha_i)L} - e^{-\operatorname{Im}(\alpha_i)L})/2 \end{aligned} \quad (23)$$

This study found that $\sin \alpha_i L$ and $\cos \alpha_i L$ include an exponential function term $e^{\operatorname{Im}(\alpha_i)L}$, and that term $e^{\operatorname{Im}(\alpha_i)L}$ diverges when the imaginary part of α_i is large, resulting in numerical errors. This problem can be solved by dividing Eq. (21) by $e^{\operatorname{Im}(\alpha_i)L}$, as follows

$$\begin{aligned} F_i &\equiv \frac{G_{1i}}{\sqrt{G_{1i}^2 + G_{2i}^2}} \left(\sin(\operatorname{Re}(\alpha_i)L) \frac{1 + e^{-2\operatorname{Im}(\alpha_i)L}}{2} + j \cos(\operatorname{Re}(\alpha_i)L) \frac{1 - e^{-2\operatorname{Im}(\alpha_i)L}}{2} \right) \\ &+ \frac{G_{2i}}{\sqrt{G_{1i}^2 + G_{2i}^2}} \left(\cos(\operatorname{Re}(\alpha_i)L) \frac{1 + e^{-2\operatorname{Im}(\alpha_i)L}}{2} - j \sin(\operatorname{Re}(\alpha_i)L) \frac{1 - e^{-2\operatorname{Im}(\alpha_i)L}}{2} \right) \\ &+ \frac{G_{3i}}{\sqrt{G_{1i}^2 + G_{2i}^2}} e^{-\operatorname{Im}(\alpha_i)L} = 0 \end{aligned} \quad (24)$$

Function F_i , which is newly defined in Eq. (24), is the constraint equation for tension estimation.

2.3 Proposed tension estimation method

As mentioned previously, Eq. (24) is the constraint equation that the natural frequency of a cable with two dampers must satisfy. The i^{th} natural frequencies f_i are not explicitly included in Eq. (24), but are implicitly included through variables α_i and β_i , as follows

$$\alpha_i = \sqrt{\sqrt{\left(\frac{T}{2EI}\right)^2 + \frac{\rho A(2\pi f_i)^2}{EI}} - \frac{T}{2EI}} \quad (25)$$

$$\beta_i = \sqrt{\sqrt{\left(\frac{T}{2EI}\right)^2 + \frac{\rho A(2\pi f_i)^2}{EI}} + \frac{T}{2EI}} \quad (26)$$

The dampers are modeled using complex springs, and thus the natural frequency f_i is also a complex value.

$$f_i = f_i^m(1 + jH_i) \tag{27}$$

where f_i^m is the real part of the complex natural frequency, and can be measured from the cable's free vibration response; H_i is the ratio of the imaginary part to the real part of the complex natural frequency, and is associated with a damping factor. However, because the damping factor is difficult to accurately measure, this study considered H_i to be unknown.

The constraint function F_i defined in Eq. (24) is a complex function, and thus Eq. (24) holds for the real and imaginary parts, respectively. Therefore, the tension and other parameters can be estimated by solving the following optimization problem.

$$\begin{aligned} & \text{minimize } y(T, EI, k_1^*, k_2^*, H_i) \\ & = \sum_{i=1}^n \left\{ \left(\text{Re}(F_i(T, EI, k_1^*, k_2^*, H_i)) \right)^2 + \left(\text{Im}(F_i(T, EI, k_1^*, k_2^*, H_i)) \right)^2 \right\} \end{aligned} \tag{28}$$

where n is the total number of natural frequencies used in the estimation. The real parts of the complex natural frequencies f_i^m ($i = 1, \dots, n$) are obtained by measurement. Density ρ , cross-sectional area A , length L , and damper positions l_1 and l_3 , are assumed to be known from design documents.

The proposed method estimates the unknowns by solving the nonlinear optimization problem in Eq. (28). The unknown values are the cable tension T , bending stiffness EI , complex spring constant k_s^* ($s = 1, 2$) of each damper, and ratio of the imaginary part of the complex natural frequency H_i ($i = 1, \dots, n$). For the dampers, the unknowns depend on the damper models. In the case of a high-damping rubber damper, the design formula for the complex spring constant is expressed as follows

$$k_s^* = ku_s + jkv_s \quad (s = 1, 2) \tag{29}$$

This study thus estimated both the real and imaginary part, ku_s and kv_s , of the complex spring constant. Each damper has two unknowns, and thus the total number of unknowns is $6 + n$ variables ($T, EI, ku_1, kv_1, ku_2, kv_2, H_i$ ($i = 1, \dots, n$)). However, because the constraint equation in Eq. (24) holds for the real and imaginary parts, the number of constraint equations is $2n$. Therefore, the number of real parts of the natural frequencies required for estimation is at least 6 ($6 + n \leq 2n$).

To solve the nonlinear optimization problem, the MultiStart method is used to prevent local optimal solutions. The MultiStart method generates multiple initial values for the parameters to be estimated. Then, the optimal solution is sought using the nonlinear least-squares method for each initial value. The optimal solution minimizing Eq. (28) is the global optimal solution. This study used 100 initial values for MultiStart method.

3. Numerical verification

3.1 Numerical models and estimation condition

Numerical simulations were conducted to validate the proposed method. The tension and other

Table 1 Numerical model parameters

(a) Cable parameters

Cable No.	Length L [m]	Tension T [kN]	Mass per unit length ρA [kg/m]	Bending stiffness EI [kN · m ²]
00	91.207	3103	34.7	274
10	104.714	2591	29.2	191
20	125.701	2856	34.7	274
30	156.541	3396	38.4	338
40	163.259	3688	47.6	527
50	183.737	3388	47.6	527
60	209.284	2489	34.7	274
70	230.991	2258	34.7	274
80	253.13	2604	38.4	338
90	287.077	4758	62.3	915

(b) Damper parameters

Damper No.	Real part of k_1^* ku_1 [kN/m]	Imaginary part of k_1^* kv_1 [kN/m]	Position of k_1^* l_1 [m]	Real part of k_2^* ku_2 [kN/m]	Imaginary part of k_2^* kv_2 [kN/m]	Position of k_2^* l_3 [m]
0	630.872	157.718	1.785	630.872	157.718	6.964
1	1369.81	342.453	1.89	1369.81	342.453	3.035
2	1452.39	363.098	2.11	1452.39	363.098	2.172
3	1540.36	385.09	2.45	1540.36	385.09	1.818
4	1914.29	478.573	2.53	1914.29	478.573	1.774
5	1914.29	478.573	2.775	1914.29	478.573	1.693
6	1011.57	252.893	4.2	1011.57	252.893	1.633
7	1011.57	252.893	4.55	1011.57	252.893	1.597
8	1000.69	250.173	4.88	1000.69	250.173	1.571
9	1346.87	336.718	5.425	1346.87	336.718	1.547

unknown parameters were estimated by inputting the real part of the complex natural frequencies obtained by the finite element method (FEM) into the proposed optimization problem (Eq. (28)). The high-damping rubber damper expressed by Eq. (29) was assumed.

By combining 10 cable models and 10 sets of two damper models, a total of 100 models were used to verify the proposed method. Tables 1(a) and 1(b) show the cable and damper specifications. The model number is the sum of the cable and damper model numbers.

The complex natural frequencies of 100 models were calculated through eigenvalue analysis in the 2-dimensional FEM. The real parts of the complex natural frequencies were used for estimation. The cables were modeled as tensioned Euler–Bernoulli beams, and the dampers were modeled as complex springs. All cable models were uniformly divided into 1200 elements, and both cable ends were fixed.

The real parts of the complex natural frequencies calculated by eigenvalue analysis were input

into Eq. (28) to obtain the optimal solution. Natural frequencies up to the eighth mode were used. The parameters to be estimated were the cable tension (T), bending stiffness (EI), real and imaginary parts of the spring constants for the two dampers (ku_1, kv_1, ku_2, kv_2), and ratio of the imaginary part to the real part of the complex natural frequency of the 1st–8th modes (H_1, \dots, H_8). Thus, a total of 14 unknowns were estimated.

3.2 Estimation results without measurement error

Fig. 2 shows the estimation results for the tension, bending stiffness, real part of the damper spring constant, and imaginary part of the damper spring constant. The horizontal axis is the model number, and the vertical axis is the ratio of the estimated value to the true value. The estimation becomes more accurate as the vertical axis approaches closer to 1.

This study confirmed that the proposed method can estimate the tension with high accuracy and maximum estimation error of 3.3 % (Fig. 2(a)). However, the bending stiffness estimation accuracy is low (Fig. 2(b)) because the bending stiffness is not sensitive to the lower-mode natural frequencies used in this estimation. Yamagiwa *et al.* (2000) proposed a method for estimating the tension and bending stiffness of a damper-free cable, and recommended using lower-mode natural frequencies for tension estimation and higher-mode natural frequencies above the 25th mode for bending stiffness estimation. However, for a cable with dampers, the higher mode quickly dissipates because of the dampers, and the higher-mode natural frequencies are difficult to estimate. Therefore, using the higher-mode natural frequencies for a cable with dampers is difficult in practice.

The estimation accuracy of the damper spring constant was low (Figs. 2(c) and 2(d)) because the estimation accuracy of the damper spring constant, k_1^* and k_2^* , depends on the estimation accuracy of the bending stiffness EI , as expressed by Eqs. (13) and (17). The estimation results for the ratio of the imaginary part to the real part of the complex natural frequency of the 1st–8th modes (H_1, \dots, H_8) are not shown, but the accuracy was also low.

The above results reveal that the proposed method can estimate the cable tension with high accuracy, but the estimation accuracy of the other parameters is low. Therefore, the proposed method should only be used for cable tension estimation. In the text below, only the tension estimation results are discussed.

3.3 Tension estimation results considering measurement error

3.3.1 Verification method

Next, the effect of measurement error on the tension estimation accuracy is considered. Tension estimation was carried out by adding a measurement error to the real part of the complex natural frequencies obtained by the FEM. The measurement error was obtained by the following equation using uniform random numbers

$$f_i^{noise} = f_i^{FEM} (1 + \varepsilon \times rand) \quad (30)$$

where f_i^{noise} is the real part of the complex natural frequency, including the measurement error; f_i^{FEM} is the real part of the complex natural frequency obtained by the FEM; $rand$ is a uniform random number in the range of -1–1; ε is the error rate. Four error rates were set from 0.005, 0.01, 0.015, and 0.02 (0.5%, 1.0%, 1.5%, and 2.0%). Model No. 00 (Cable model: No. 0, Damper

model: No. 0) was used for verification. Ten patterns of a set of the 1st-8th natural frequencies, including the measurement error for each error rate ε , were created and used for verification. For each error rate, two error indices, namely, the root mean square error ratio (RMSER), and maximum error ratio (MER), defined by Eqs. (31) and (32) were calculated using the estimation results for 10 patterns.

$$RMSER = \sqrt{\frac{1}{N} \sum_{I=1}^N \left(\frac{T_I^{noise}}{T^{true}} - 1 \right)^2} \quad (31)$$

$$MER = \max \left(\left| \frac{T_I^{noise}}{T^{true}} - 1 \right| \right) \quad (32)$$

where $N = 10$, T_I^{noise} is the estimated tension of the I^{th} pattern, and T^{true} is the true tension.

3.3.2 Estimated results

The relationship between the measurement error rate ε and two error indices (RMSER, MER) is shown in Fig. 3. This result indicates that the proposed method can estimate the tension with an average error of 5% and maximum error of up to 7% when the natural frequency contains an error rate of 2%. The tension estimation error of the higher-order vibration method for a damper-free cable has been reported as 5% (Shinko Wire Company, 2021), and thus the proposed method may have sufficient accuracy because it does not require removing and reinstalling the dampers.

4. Experimental verification

4.1 Experiment overview

Next, the proposed method was validated experimentally. A schematic diagram and photograph of the test specimen are shown in Fig. 4. The cable was tensioned and fixed at both ends. The cable tension measured with a load cell was considered as the true value. Free vibration was induced by hitting the cable with a hammer, and the acceleration histories were measured using two accelerometers. The acceleration histories were Fourier-transformed, and the natural frequencies were obtained by reading the frequencies at which the Fourier amplitude was predominant.

The cable specifications are presented in Table 2(a), and the damper specifications are presented in Table 2(b). The damper was fabricated using a high-damping rubber damper. The spring constants of the dampers were obtained by cyclic loading tests with the three loading frequencies of 1 Hz, 2 Hz, and 3 Hz, and four loading displacements of 0.25 mm, 0.5 mm, 1.0 mm, and 1.5 mm. Table 2(b) presents the averaged values.

The experimental cases are presented in Table 3. Experiments were conducted on 29 cases with three different tension values (approximately 20 kN, 30 kN, or 60 kN), different number of dampers (0, 1, or 2 dampers), and different damper locations. Cases 1–3 are the cases without damper and Cases 4–10 are cases with one damper. Two dampers were used in all other cases. Table 3 presents the measured natural frequencies in ascending order. The natural frequencies for which the peak of the Fourier spectrum is unclear are left blank.

First, as an example, the acceleration time histories and acceleration Fourier spectra for Cases 1,

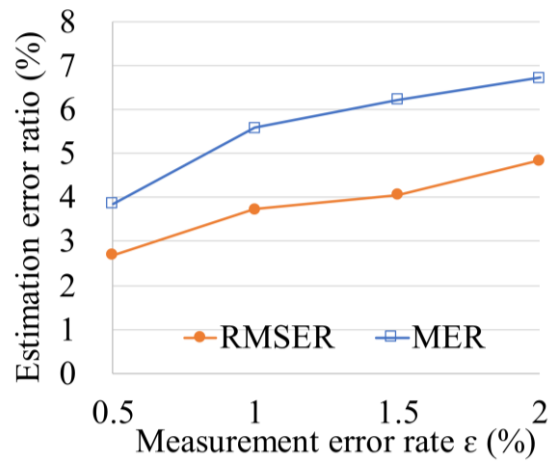
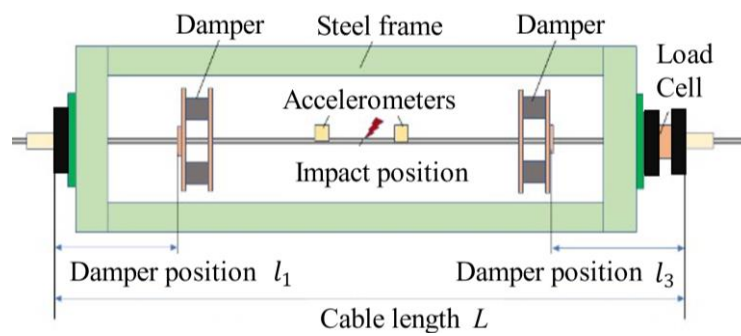


Fig. 3 Relationship between measurement error rate in natural frequency and tension estimation error ratio



(a) Schematic diagram of test specimen, impact position, and measurement locations



(b) Photo of test specimen

Fig. 4 Schematic diagram and photo of test specimen

5, and 11, wherein the tension is approximately 20 kN, are shown in Fig. 5. Case 1 is the case without a damper, Case 5 is the case with one damper, and Case 11 is the case with two dampers.

Table 2 Test specimen parameters

(a) Cable parameters

Length (measured value)	Mass per unit length (catalog value)	Bending stiffness (design value)
L [m]	ρA [kg/m]	EI [kN · m ²]
6.731	1.113	0.257

(b) Damper parameters (spring constants obtained by element tests; masses obtained by measurement)

Real part of k_1^*	Imaginary part of k_1^*	Mass of k_1^*	Real part of k_2^*	Imaginary part of k_2^*	Mass of k_2^*
ku_1 [kN/m]	kv_1 [kN/m]	m_1 [kg]	ku_2 [kN/m]	kv_2 [kN/m]	m_3 [kg]
21.3	13.	0.4665	21.3	13.0	0.4714

Table 3 Experimental cases and measured natural frequencies

Case No.	Cable Tension T (load cell) [kN]	Damper Position		Measured natural frequencies [Hz] (ascending order)								
		l_1 [m]	l_3 [m]	1st	2nd	3rd	4th	5th	6th	7th	8th	9th
1	19.61	-	-	10.2	20.38	30.8	41.64	52.85	64.37	76.77	89.49	102.9
2	31.32	-	-	12.85	25.59	38.55	51.79	65.6	79.39	93.98	109	124.8
3	60.74	-	-	17.66	35.2	52.93	71.05	89.57	108	126.8	146.4	165.9
4	19.4	370	-	10.63	21.17	31.28	38.93	50.53	63.1	75.84	89.49	106.3
5	19.53	520	-	10.7	21.2	30.72	47.23	58.47	71.33	84.58	98.51	113.1
6	19.53	670	-	10.94	21.6	30.53	48.09	60.04	73.03	86.82	101.4	116.4
7	31.33	370	-	13.09	25.89	37.18	56.77	71.09	85.5	100.62	116.22	132.68
8	31.07	520	-	13.28	26.09	36.44	57.95	72.38	87.32	103.07	119.33	136.02
9	31.27	670	-	13.59	26.5	36.25	46.39	59.52	74.25	89.73	106.18	123.2
10	60.74	663	-	17.7	38.47	57.79	77.82	98.67	121.34	143.11	164.07	185.17
11	19.4	370	453	10.87	21.71	31.91	40.28	53.05	63.62	76.21	89.52	103.9
12	19.4	370	563	11.05	21.99	32.18	40.17	53.61	64.53	77.29	91.23	106.3
13	19.4	370	673	11.25	22.36	32.61	40.5	54.66	65.77	78.9	93.15	108.7
14	19.6	520	453	11.2	22.15	31.73	45.88	53.61	65.3	78.47	92.87	108.1
15	19.6	520	563	11.4	22.48	32.05	44.99	53.98	66.2	79.89	94.71	110.3
16	19.6	520	673	11.6	22.84	32.36	45.03	54.68	67.37	81.52	96.73	112.6
17	19.53	670	453	11.45	22.55	31.39	46.29	54.39	66.62	80.48	95.59	111.4
18	19.53	670	563	11.59	22.82	31.88	-	54.82	67.54	81.82	97.27	113.5
19	19.47	670	673	11.83	23.21	32.16	46.06	55.56	68.88	83.6	99.44	115.8
20	31.27	370	453	13.73	27.1	38.82	53.92	66.73	77.29	92.36	108.81	126.07
21	31.13	370	563	13.68	26.76	37.57	52.39	64.7	78.69	94.41	111.07	128.49
22	31.08	370	673	13.91	27.09	37.7	52.66	65.55	80.09	96.36	113.39	131.23
23	31.07	520	453	13.76	26.79	36.59	53.01	65.11	79.37	95.57	112.48	130.23
24	31.07	520	563	13.95	27.05	37.22	52.75	65.81	80.54	97.31	114.57	132.71
25	31.13	520	673	14.19	27.36	37.41	53.01	66.84	82.25	99.27	117.04	135.37
26	31.07	670	453	14.04	27.05	36.44	53.84	66.34	81.39	98.24	116.03	134.27
27	31.07	670	563	14.25	27.35	36.61	53.73	67.23	82.78	100.09	118.33	136.87
28	31.27	670	673	14.5	27.76	36.9	54.07	68.3	84.65	102.42	121.1	139.86
29	60.74	663	663	20.72	42.06	64.11	86.11	115	138.8	162.33	184.66	207.23

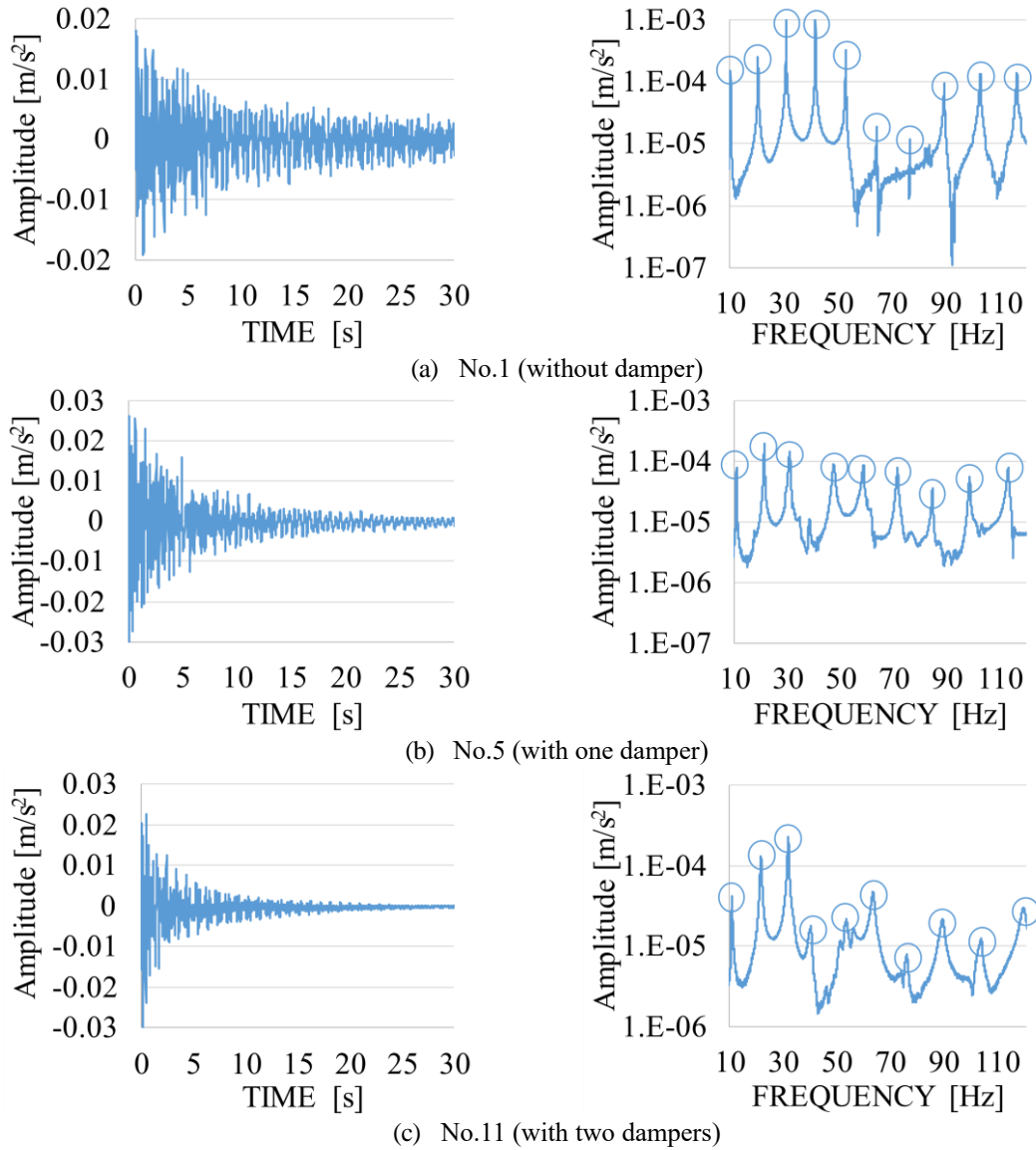


Fig. 5 Acceleration time history and Fourier spectrum for cases with approximately 20 kN tension

The frequencies corresponding to circles in the acceleration Fourier spectrum were read as natural frequencies. As the number of dampers increased, the amplitude of the acceleration time history decayed faster, the amplitude of the higher modes in the Fourier spectrum became smaller, and the shape of the Fourier spectrum around the peaks became slightly smoother. This indicates that higher modes decay faster and are more difficult to measure as the number of dampers increases. However, as shown in Fig. 5, it was possible to read at least 10 natural frequencies even with two dampers, which is sufficient for tension estimation using the proposed method.

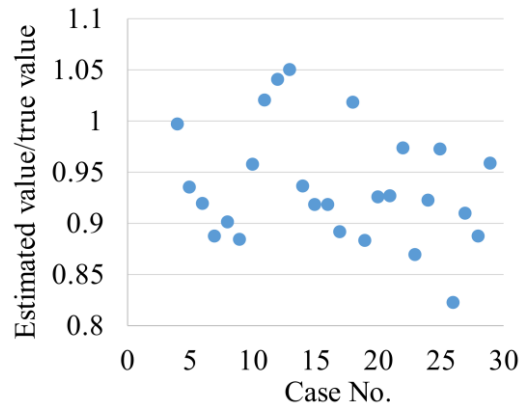


Fig. 6 Ratio of estimated tension to true tension using damper design formula (Eq.(33))

Table 4 Comparison of average measured natural frequencies with values calculated by FEM [Hz] (No. 11)

	1st	2nd	3rd	4th	5th	6th	7th	8th	9th	
FEM (Eq. (33))	10.42	20.79	31.05	41.06	50.76	60.41	70.55	81.66	93.95	
Measurement	10.87	21.71	31.91	40.28	53.05	63.62	76.21	89.52	103.9	
FEM (Eq. (34))	10.42	20.87	31.44	42.33	51.15	56.60	65.45	75.80	89.37	103.8
	1st	2nd	3rd	4th	5th	6th	7th	8th	9th	10th

4.2 Tension estimation result

4.2.1 Tension estimation using design formula for high-damping rubber damper

The measured natural frequencies up to the eighth mode were input into the proposed method. To model the dampers, the design formula for the high-damping rubber damper expressed by Eq. (29) was used because the dampers of the test specimen were created using high-damping rubber.

The mass of damper was considered by introducing the inertia force term, as follows

$$\text{Design damper formula: } k_s^* = -(2\pi f_i)^2 m_s + ku_s + jkv_s \quad (33)$$

where m_s is the mass of the damper s ; the values listed in Table 2(b) were used.

For the cases with one damper, the damper spring constant k_2^* was assumed to be zero. For the cases without dampers, only the cable's tension and bending stiffness were estimated, assuming that the spring constants of the two dampers are zero.

The estimation results are shown in Fig. 6. Case 26 has a large estimation error of 17%. The authors considered that the tension estimation accuracy was low because the damper design formula does not accurately represent the behavior of the dampers.

4.2.2 Measured natural frequencies and natural frequencies calculated by FEM

The natural frequencies of Case 11 (with two dampers) were calculated using eigenvalue analysis with the cable specifications listed in Table 2(a) and damper specifications listed in Table

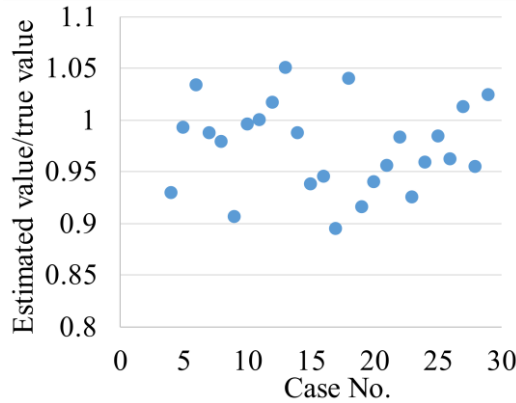


Fig. 7 Ratio of estimated tension to true tension using refined damper formula (Eq.(34))

Table 5 Tension estimation error for different damper formulas

Number of dampers	Root Mean Square Error Ratio (RMSER)		Maximum Error Ratio (MER)	
	Damper formula		Damper formula	
	Design (Eq. (33))	Refined (Eq. (34))	Design (Eq. (33))	Refined (Eq. (34))
1	8.28%	4.73%	11.6%	9.4%
2	8.48%	4.99%	17.7%	10.5%

2(b). The “FEM (Eq. (33))” row in Table 4 contains the values calculated using the damper model expressed by Eq. (33). The “Measurement” row includes the measured natural frequencies. The “FEM (Eq. (33))” and “Measurement” rows are in good agreement from the first to the fourth order. However, the difference increases above the fifth order, and Eq. (33) underestimates the natural frequencies. Because cable dampers are typically used to suppress low-frequency vibrations, it is assumed that the damper design formula does not accurately represent the behavior of dampers.

On the basis of the above-mentioned observation, and through trial and error, this study refined the damper formula by adding an imaginary term that increases with the frequency, as follows

$$\text{Refined damper formula: } k_s^* = -(2\pi f_i)^2 m_s + k u_s + j\{k v_s + (2\pi f_i)^2 c_s\} \quad (34)$$

where c_s is the new variable. The natural frequencies were calculated by substituting 0.0006 into c_s for both dampers. The row of “FEM (Eq. (34))” in Table 4 is the natural frequency calculated using Eq. (34). “Measurement” and “FEM (Eq. (34))” are in good agreement from the first to the fourth order. The 6th to 9th order of “Measurement” are in good agreement with the 7th to 10th order of “FEM (Eq. (34)).” Equation (34) cannot express 53.05 Hz. However, Eq. (34) can express almost all other measured natural frequencies. Therefore, this study considered Eq. (34) as the refined damper model.

4.2.3 Tension estimation using refined damper model

Next, the refined damper model was used for tension estimation. Because the refined damper

model has two additional unknowns (c_s , $s = 1, 2$), the 1st–9th natural frequencies were used such that the constraint equations were more than the number of unknowns.

Fig. 7 shows the tension estimation results obtained using the refined damper model. The maximum error is approximately 10%, and the accuracy improved when the refined damper model was used.

4.3 Discussion

Table 5 compares the tension estimation accuracy using two error indices (RMSE, MER) between the case wherein the damper design formula of Eq. (33) was used and the case wherein the refined damper formula of Eq. (34) was used for each damper amount. The two damper models have larger error indices compared with the single damper model, owing to the higher number of errors in the damper modeling. The tension estimation error was reduced by using the refined damper formula, particularly when a cable has two dampers. Using the refined damper formula, the RMSE were within 5%, and the MER was approximately 10%, even with two dampers. Therefore, appropriate damper modeling is crucial, particularly when carrying out tension estimation for a cable with two dampers.

5. Conclusions

This study developed a tension estimation method for cables with two dampers. The proposed method was numerically and experimentally validated. The following conclusions were drawn from this study.

The cable was modeled as a tensioned Euler–Bernoulli beam, and a constraint equation for tension estimation was derived from the vibration equation and boundary conditions. The tension was estimated by substituting the real part of the complex natural frequency into the constraint equation for various modes and solving an optimization problem. The cable bending stiffness, damper spring constant, and ratio of the imaginary part to the real part of the complex natural frequency were estimated in addition to the cable tension.

In the numerical verification, the sets of natural frequencies calculated by the finite element method were used for estimation. The tension was estimated accurately with an estimation error within 3.3% for all 100 models. However, the accuracy of the other parameters was low, indicating that the proposed method is only practical for tension estimation. The effect of the measurement error in the natural frequencies was also investigated, and it was found that the proposed method has sufficient accuracy even when the measurement error rate is 2%.

In the experimental verification, a 6.731-m cable model and a damper model made of high-damping rubber was used. The cable tension measured by a load cell was used as the true tension value. First, the cable tension was estimated using the design formula of the high-damping rubber damper. However, the tension estimation accuracy was low, and the maximum error was approximately 18%. The eigenvalue analysis revealed that the numerical and measured natural frequencies are in good agreement for the lower modes, but the difference was negligible for the higher modes. Therefore, it is considered that the design formula of the high-damping-rubber damper did not accurately express the characteristics of higher modes. Therefore, the damper model was refined by introducing the imaginary term proportional to the square of the frequency. Finally, the refined damper model was used, and the proposed method could estimate the tension

with a maximum error of approximately 10%.

The tension estimation error between the design damper formula and the refined damper formula was compared for cases with one damper and cases with two dampers. The two-damper models have larger error indices compared with the single damper model, owing to the higher number of errors in the damper modeling. Therefore, appropriate damper modeling is crucial, particularly for a cable with two dampers. By using the refined damper model, the tension estimation error was reduced. Particularly, the introduction of the refined damper formula greatly reduced the estimation error for the two-damper cases.

The main achievements of this study can be summarized as follows. This study has successfully developed an accurate tension estimation method for a cable equipped with two dampers based on natural frequency measurements. The proposed method makes it possible to estimate the tension without removing the dampers, and contributes to reducing the effort and time of the inspection work. This study also pointed out the necessity of the damper formula for the purpose of tension estimation, and the process of developing the damper formula was demonstrated. This study not only introduces a novel tension estimation method but also addresses a key issue in the damper design formula, ultimately leading to a more accurate tension estimation for cables equipped with two dampers.

Future work should develop a tension estimation method that is not affected by the damper modeling error.

Acknowledgments

We thank Edanz (<https://jp.edanz.com/ac>) for editing a draft of this manuscript.

References

- Chen, C.C., Wu, W.H., Leu, M.R. and Lai, G. (2016), "Tension determination of stay cable or external tendon with complicated constraints using multiple vibration measurements", *Measurement*, **86**, 182-195. <https://doi.org/10.1016/j.measurement.2016.02.053>.
- Chen, C.C., Wu, W.H., Leu, M.R. and Lai, G. (2018), "A novel tension estimation approach for elastic cables by elimination of complex boundary condition effects employing mode shape functions", *Eng. Struct.*, **166**, 152-166. <https://doi.org/10.1016/j.engstruct.2018.03.070>.
- Feng, Z., Wang, X. and Chen, Z. (2010), "A method of fundamental frequency hybrid recognition for cable tension measurement of cable-stayed bridges", *Proceedings of the 8th IEEE International Conference on Control and Automation*. <https://doi.org/10.1109/ICCA.2010.5524186>.
- Foti, F., Geuzaine, M. and Denoel, V. (2020), "On the identification of the axial force and bending stiffness of stay cables anchored to flexible supports", *Appl. Math. Model.*, **92**, 798-828. <https://doi.org/10.1016/j.apm.2020.11.043>.
- Furukawa, A., Hirose, K. and Kobayashi, R. (2021a), "Tension estimation method for cable with damper using natural frequencies", *Front. Built Environ.*, **7**(603857), <https://doi.org/10.3389/fbuil.2021.603857>.
- Furukawa, A., Hirose, K. and Kobayashi, R. (2022b), "Tension estimation method for cable with damper and its application to real cable-stayed bridge", (Eds., Wu, Z., Nagayama, T., Dang, J. and Astroza, R.) *Experimental Vibration Analysis for Civil Engineering Structures. Lecture Notes in Civil Engineering*, **224**. https://doi-org.kyoto-u.idm.oclc.org/10.1007/978-3-030-93236-7_32
- Furukawa, A., Kozuru, K. and Kobayashi, R. (2022c), "Method for estimating tension of two Nielsen–Lohse bridge cables with intersection clamp connection and unknown boundary conditions", *Front. Built*

- Environ.*, **8**(906871). <https://doi.org/10.3389/fbuil.2022.993958>.
- Furukawa, A., Suzuki, S. and Kobayashi, R. (2022d), “Tension estimation method for cable with damper using natural frequencies with uncertain modal order”, *Front. Built Environ.*, **8**(812999). <https://doi.org/10.3389/fbuil.2022.812999>.
- Furukawa, A., Suzuki, S. and Kobayashi, R. (2022e), “Tension estimation method for cable with damper using natural frequencies and two-point mode shapes with uncertain modal order”, *Front. Built Environ.*, **8**(906871). <https://doi.org/10.3389/fbuil.2022.906871>.
- Furukawa, A., Yamada, S. and Kobayashi, R. (2022f), “Tension estimation methods for two cables connected by an intersection clamp using natural frequencies”, *J. Civ. Struct. Health Monit.*, **12**, 339-360. <https://doi.org/10.1007/s13349-022-00548-6>.
- Furukawa, A., Yamada, S. and Kobayashi, R. (2022g), “Tension estimation methods for Nielsen-Lohse bridges using out-of-plane and in-plane natural frequencies”, *Int. J. Geomate*, **23**(97), 1-11. <https://doi.org/10.21660/2022.97.3235>.
- Gan, Q., Huang, Y., Wang, R.O. and Rao, R. (2019), “Tension estimation of hangers with shock absorber in suspension bridge using finite element method”, *J. Vibroeng.*, **21**(3), 587-601. <https://doi.org/10.21595/jve.2018.20054>.
- Hou, J., Li, C., Jankowski, L., Shi, Y., Su, L., Yu, S. and Geng, T. (2020), “Damage identification of suspender cables by adding virtual supports with the substructure isolation method”, *Struct. Control Health Monit.*, **28**(3), e2677, <https://doi.org/10.1002/stc.2677>.
- Izzi, M., Caracogilia, L. and Noe, S. (2016), “Investigating the use of Targeted-Energy-Transfer devices for stay-cable vibration mitigation”, *Struct. Control Health Monit.*, **23**, 315-332. <https://doi.org/10.1002/stc.1772>.
- Javanbakht, M., Cheng, S. and Ghrib, F. (2019), “Control-oriented model for the dynamic response of a damped cable”, *J. Sound Vib.*, **442**, 249-267. <https://doi.org/10.1016/j.jsv.2018.10.036>.
- Jeong, S., Kim H., Lee, J. and Sim, S.H. (2020), “Automated wireless monitoring system for cable tension force using deep learning”, *Struct. Health Monit.*, **20**(4), 1805-1821. <https://doi.org/10.1177/1475921720935837>.
- Kim, B.H. and Park, T. (2007), “Estimation of cable tension force using the frequency-based system identification method”, *J. Sound Vib.*, **304**, 660-676. <https://doi.org/10.1016/j.jsv.2007.03.012>.
- Krenk, S. (2000), “Vibration of a taut cable with an external damper”, *ASME, J. Appl. Mech.*, **67**, 772-776. <https://doi.org/10.1115/1.1322037>.
- Lazar, I.F., Neild, S.A. and Wagg, D.J. (2016), “Vibration suppression of cables using tuned inerter dampers”, *Eng. Struct.*, **122**, 62-71. <https://doi.org/10.1016/j.engstruct.2016.04.017>.
- Li, S., Wang, L., Wang, H., Shi, P., Lan, R., Wu, C. and Wang, X. (2021), “An accurate measurement method for tension force of short cable by additional mass block”, *Adv. Mater. Sci. Eng.*, **2021**(6622628), <https://doi.org/10.1155/2021/6622628>.
- Liu G., Wang, X., Wang, X., Wan, Y. and Li, B. (2023), “Noncontact cable tension estimation using edge recognition technology based on convolutional network”, *Structures*, **58**(105337). <https://doi-org.kyoto-u.idm.oclc.org/10.1016/j.istruc.2023.105337>.
- Ma, L. (2017), “A highly precise frequency-based method for estimating the tension of an inclined cable with unknown boundary conditions”, *J. Sound Vib.*, **409**, 65-80. <https://doi.org/10.1016/j.jsv.2017.07.043>.
- Ma, L., Xu, H., Munkhbaatar, T. and Li, S. (2021), “An accurate frequency-based method for identifying cable tension while considering environmental temperature variation”, *J. Sound Vib.*, **490**(115693). <https://doi.org/10.1016/j.jsv.2020.115693>.
- MathWorks. (2024), MATLAB Documentation, MultiStart. <https://jp.mathworks.com/help/gads/multistart.html>. [Accessed: January 30, 2024].
- Pacheco, B.M., Fujino, Y. and Sulekh, A. (1993), “Estimation curve for modal damping in stay cables with viscous damper”, *J. Struct. Eng.*, **119**(6), 1961-1979. [https://doi.org/10.1061/\(ASCE\)0733-9445\(1993\)119:6\(1961\)](https://doi.org/10.1061/(ASCE)0733-9445(1993)119:6(1961)).
- Shan, D., Zhou, X. and Khan, I. (2019), “Tension identification of suspenders with supplemental dampers for through and half-through arch bridges under construction”, *ASCE, J. Struct. Eng.*, **145**(3), Paper ID

04018265. [https://doi.org/10.1061/\(ASCE\)ST.1943-541X.0002255](https://doi.org/10.1061/(ASCE)ST.1943-541X.0002255).
- Shi, X. and Zhu, S. (2018), “Dynamic characteristics of stay cables with inerter dampers”, *J. Sound Vib.*, **423**, 287-305. <https://doi.org/10.1016/j.jsv.2018.02.042>.
- Shinke, T., Hironaka, K., Zui, H. and Nishimura, H. (1980), “Practical formulas for estimation of cable tension by vibration method”, *J. Jpn Soc. Civil Engineers*, **294**, 25-32. (In Japanese) https://doi.org/10.2208/jscej1969.1980.294_25.
- Shinko Wire Company, Ltd. (2020), Tension measuring technique for outer cables. <http://www.shinko-wire.co.jp/products/vibration.html>. [Accessed: January 30, 2024]. (In Japanese)
- Tabatabai, H. and Mehrabi, B. (2000), “Design of mechanical viscous dampers for stay cables”, *J. Bridge Eng. ASCE*, **5**(2), 114-123. [https://doi.org/10.1061/\(ASCE\)1084-0702\(2000\)5:2\(114\)](https://doi.org/10.1061/(ASCE)1084-0702(2000)5:2(114)).
- Thyagarajan, S.K., Schulz, M.J. and Pai, P.F. (1998), “Detecting structural damage using frequency response functions”, *J. Sound Vib.*, **210**, 162-170. <https://doi.org/10.1006/jsvi.1997.1308>.
- Weber, F. and Distl, H. (2015), “Amplitude and frequency independent cable damping of Sutong Bridge and Russky Bridge by magnetorheological dampers”, *Struct. Control Health Monit.*, **22**(2), 237-254. <https://doi.org/10.1002/stc.1671>.
- Yamagiwa, I., Utsuno, H., Endo, K. and Sugii, K. (2000), “Identification of flexural rigidity and tension of one-dimensional structure by measuring eigenvalues in higher order”, *T. Jpn Soc. Mech. Engineers*, **66**(649), 2905-2911. (In Japanese). <https://doi.org/10.1299/kikaic.66.2905>.
- Yan, B., Chen, W., Dong, Y. and Jiang, X. (2020), “Tension force estimation of cables with two intermediate supports”, *Int. J. Struct. Stab. Dyn.*, **20**(3), Paper ID 2050032, <https://doi.org/10.1142/S0219455420500327>.
- Yan, B., Chen, W., Yu, J. and Jiang, X. (2019), “Mode shape-aided tension force estimation of cable with arbitrary boundary conditions”, *J. Sound Vib.*, **440**, 315-331. <https://doi.org/10.1016/j.jsv.2018.10.018>.
- ZarbaF, S.E.H.A.M., Norouzi, M., Allemang, R., Hunt, V. and Helmicki, A. (2017), “Stay cable tension estimation of cable-stayed bridges using genetic algorithm and particle swarm optimization”, *J. Bridge Eng.*, **22**(10), Paper ID 05017008. [https://doi.org/10.1061/\(ASCE\)BE.1943-5592.0001130](https://doi.org/10.1061/(ASCE)BE.1943-5592.0001130).
- ZarbaF, S.E.H.A.M., Norouzi, M., Allemang, R., Hunt, V., Helmicki, A. and Venkatesh, C. (2018), “Vibration-based cable condition assessment: A novel application of neural networks”, *Eng. Struct.*, **177**, 291-305. <https://doi.org/10.1016/j.engstruct.2018.09.060>.
- Zui, H., Sinke, T. and Namita, Y. (1996), “Practical formulas for estimation of cable tension by vibration method”, *J. Struct. Eng. ASCE*, **122**(6), 651-656. [https://doi.org/10.1061/\(ASCE\)0733-9445\(1996\)122:6\(651\)](https://doi.org/10.1061/(ASCE)0733-9445(1996)122:6(651)).